Correlation and scaling behaviors of fine particulate matter (PM 2.5) concentration in China

5 authors, including:

Yongwen Zhang
Bar Ilan University
11 PUBLICATIONS **7** CITATIONS

SEE PROFILE

Jingfang Fan
Potsdam Institute for Climate Impact Research
34 PUBLICATIONS **108** CITATIONS

SEE PROFILE

Shlomo Havlin
Bar Ilan University
987 PUBLICATIONS **62,559** CITATIONS

SEE PROFILE

Some of the authors of this publication are also working on these related projects:

Project   Network Reliability View project

Project   Semantic networks and creativity View project

LETTER

Correlation and scaling behaviors of fine particulate matter (PM$_{2.5}$) concentration in China

To cite this article: Yongwen Zhang *et al* 2018 *EPL* **122** 58003

View the article online for updates and enhancements.

Correlation and scaling behaviors of fine particulate matter (PM$_{2.5}$) concentration in China

Yongwen Zhang[1,2], Dean Chen[3], Jingfang Fan[4], Shlomo Havlin[4] and Xiaosong Chen[2,5(a)]

[1] *Data Science Research Center, Faculty of Science, Kunming University of Science and Technology Kunming 650500, Yunnan, China*
[2] *CAS Key Laboratory of Theoretical Physics, Institute of Theoretical Physics, Chinese Academy of Sciences P. O. Box 2735, Beijing 100190, China*
[3] *Department of Physics, University of Helsinki - P.O. Box 48, 00014 Helsinki, Finland*
[4] *Department of Physics, Bar-Ilan University - Ramat-Gan 52900, Israel*
[5] *School of Physical Sciences, University of Chinese Academy of Sciences - Beijing 100049, China*

Abstract – Air pollution has become a major issue and caused widespread environmental and health problems. Aerosols or particulate matters are an important component of the atmosphere and can transport under complex meteorological conditions. Based on the data of $PM_{2.5}$ observations, we develop a network approach to study and quantify their spreading and diffusion patterns. We calculate cross-correlation functions of the time lag between sites within different seasons. The probability distribution of correlation changes with season. It is found that the probability distributions in four seasons can be scaled into one scaling function with averages and standard deviations of correlation. This seasonal scaling behavior indicates that there is the same mechanism behind correlations of $PM_{2.5}$ concentration in different seasons. Further, the weighted degrees reveal the strongest correlations of $PM_{2.5}$ concentration in winter and in the North China Plain for the positive correlation pattern that is mainly caused by the transport of $PM_{2.5}$. These directional degrees show net influences of $PM_{2.5}$ along Gobi and inner Mongolia, the North China Plain, Central China, and Yangtze River Delta. The negative correlation pattern could be related to the large-scale atmospheric waves.

Introduction. – Aerosols or particulate matters, which control the process from low visibility events to precipitation, are important components of the atmosphere. They play a critical role in the global climate pattern and public health. Chen *et al.* [1] have reported the impact on life expectancy of sustained exposure to air pollution from China's Huai River policy. Due to anthropogenic emissions, the concentration of particulate matters is growing sharply. In the past few years, China has witnessed a rapid growth both in industry and in cities population. As a result, air pollution, especially the pollution caused by the high fine particulate matter (*i.e.*, with aerodynamic diameters not larger than 2.5 μm, or $PM_{2.5}$) concentration, has become a serious issue [2].

Most previous studies on $PM_{2.5}$ concentrated on observation in one site. Winter and summer $PM_{2.5}$ chemical compositions in 14 cities of China have been analysed by Cao *et al.* [3]. The publication of hourly data since 2013 provided the possibility to study the spatial distribution and seasonal variation of $PM_{2.5}$ in China [4]. Using the monitoring data in the North China Plain and the Yangtze River Delta, Hu *et al.* [5] found a strong temporal correlation between cities within 250 km. For 81 cities in China, Gao *et al.* [6] studied air pollution of city clusters from June 2004 to June 2007. The relation between the air quality over Beijing and its surroundings and circulation patterns was studied by Zhang *et al.* [7]. The spatiotemporal variations of $PM_{2.5}$ and PM_{10} concentrations of 31 Chinese cities from March 2013 to March 2014 were related to SO_2, NO_2, CO and O_3 [8]. At a suburban site

---

[a]E-mail: `chenxs@itp.ac.cn`

between Beijing and Tianjin, the correlation of pollutants with meteorological conditions was discussed [9].

The studies [5,6] have shown that $PM_{2.5}$ concentrations in different cities are not localized and related to each other. It is of great interest to investigate how far the $PM_{2.5}$ concentrations in different cities of China are correlated. Using the hourly data of monitoring sites over China, the spatial correlations of $PM_{2.5}$ concentrations in 2015 have been studied using the principal component analysis [10].

In the last decade, networks have emerged as an important tool in studies of complex systems and has been applied to a wide variety of disciplines [11–13]. Recently, complex network theory has been used to study climate systems [14–21]. For a climate system, geographical locations or grid points are regarded as nodes of network and the links between them are defined by a cross-correlation function [18,21] or other ways like event synchronization [22,23], mutual information [24,25] and causalities [26].

In this letter, we study the global properties of $PM_{2.5}$ concentrations in China from the aspect of complex networks. The nodes of $PM_{2.5}$ concentration network can be defined from the monitoring stations. Using $PM_{2.5}$ concentration data, we can calculate the correlation between nodes and define their links. Our work is organized as follows. In the next section, we describe the data and introduce the methodology. The results are presented and discussed in the third section. Finally, a short summary is given.

Data and methodology. –

Data. The Ministry of Environmental Protection of China has been publishing the air quality index since 2013 and has provided data for us to study atmospheric pollution. We use the hourly $PM_{2.5}$ concentration data of 754 monitoring sites over China from Dec. 2014 to Nov. 2015 (http://113.108.142.147:20035/emcpublish/). In pre-processing, we transform 754 monitoring stations into 163 sites with an area $1° \times 1°$. The concentration of a site is defined by the average of monitoring stations inside this site. Since the strong seasonal dependence of $PM_{2.5}$ concentration, we divide the data into four groups corresponding to winter (Dec., Jan., Feb.), spring (Mar., Apr., May), summer (Jun., Jul., Aug.) and autumn (Sep., Oct., Nov.).

Methodology. During a time period T, the $PM_{2.5}$ concentration of site i is represented by a series $X_i(t)$. With respect to its average $\langle X_i \rangle = \frac{1}{T} \sum_{t=1}^{T} X_i(t)$, there is a fluctuation series $\delta X_i(t) = X_i(t) - \langle X_i \rangle$. To study the correlation of $PM_{2.5}$ concentration between sites i and j, we calculate the cross-correlation function [18]

$$\hat{C}_{ij}(\tau) = \frac{\langle \delta X_i(t) \cdot \delta X_j(t+\tau) \rangle}{\sqrt{\langle [\delta X_i(t)]^2 \rangle} \cdot \sqrt{\langle [\delta X_j(t+\tau)]^2 \rangle}}, \quad (1)$$

where $-\tau_{max} \leq \tau \leq \tau_{max}$ is the time lag. On the basis of time-reversal symmetry, there is a relation $\hat{C}_{ij}(-\tau) = \hat{C}_{ji}(\tau)$. The cross-correlation in the interval $[-\tau_{max}, \tau_{max}]$ can be calculated by $\hat{C}_{ij}(\tau \geq 0)$ and $\hat{C}_{ji}(\tau \geq 0)$. We identify the largest absolute value of $\hat{C}_{ij}(\tau)$ and denote the corresponding time lag as τ_{ij}^*. The correlation between sites i and j is defined as $C_{ij} \equiv \hat{C}_{ij}(\tau^*)$. If $\tau_{ij}^* \neq 0$, the correlation between sites i and j is directional. The direction of correlation is from i to j when $\tau_{ij}^* > 0$ and from j to i when $\tau_{ij}^* < 0$.

For given N nodes, there are $(N-1)N/2$ correlations and they can be described by a probability distribution function (PDF) $\rho(C)$.

For the definition of a network, a threshold Δ of correlation is introduced to exclude noise. The adjacency matrix of the network is defined with the threshold as

$$A_{ij} = \begin{cases} 1 - \delta_{ij}, & |C_{ij}| > \Delta, \\ 0, & |C_{ij}| \leq \Delta, \end{cases} \quad (2)$$

where Kronecker's delta $\delta_{ij} = 0$ for $i \neq j$ and $\delta_{ij} = 1$ for $i = j$ so that self-loops are excluded.

The importance of site i in the network is characterized usually by its degree $k_i^C = \sum_{j=1}^{N} A_{ij}$ [11]. More information can be taken into account with a weighted degree

$$\bar{k}_i^C = \sum_{j=1}^{N} A_{ij} |C_{ij}|. \quad (3)$$

The direction from sites i to j is described by a unit vector $\vec{e}_{ij} = \frac{1}{d}(\delta\phi, \delta\theta)$ with $d = \sqrt{\delta\phi^2 + \delta\theta^2}$, where $\delta\phi$ and $\delta\theta$ are the longitude and latitude differences of i and j, respectively. We can further introduce a directional degree as

$$\vec{k}_i^C = \sum_{j=1, \tau_{ij}^*>0}^{N} A_{ij}|C_{ij}|\, \vec{e}_{ij} + \sum_{j=1, \tau_{ij}^*<0}^{N} A_{ij}|C_{ij}|\, (-\vec{e}_{ij}) \quad (4)$$

to quantify the $PM_{2.5}$ concentration directional influences of site i.

Alternatively, we can determine network links according to

$$G_{ij} = \frac{C_{ij} - \text{mean}(\hat{C}_{ij}(\tau))}{\text{std}(\hat{C}_{ij}(\tau))}, \quad (5)$$

where "mean" and "std" represent the mean and standard deviation of the cross-correlation function [19,27,28]. G_{ij} characterizes actually the significance of the correlation C_{ij} among $\hat{C}_{ij}(\tau)$ of different time lag τ.

The adjacency matrix of the network is now defined as

$$B_{ij} = \begin{cases} 1 - \delta_{ij}, & |G_{ij}| > \Theta, \\ 0, & |G_{ij}| \leq \Theta \end{cases} \quad (6)$$

with the threshold Θ of G. With C_{ij} replaced by G_{ij} in eq. (3) and eq. (4), we can obtain the weighted degree $\bar{k}_i^G$ and the directional degree $\vec{k}_i^G$ of G.
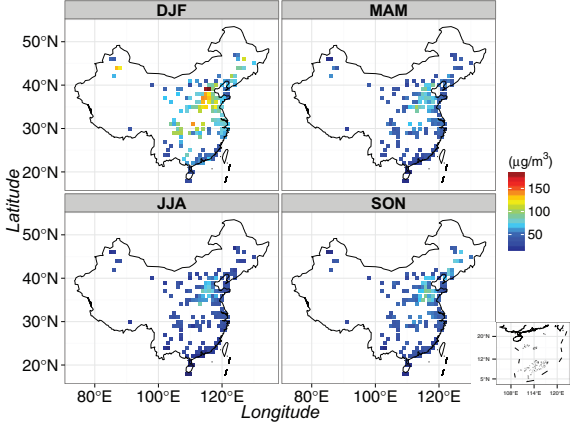
Fig. 1: (Color online) Distribution of mean $PM_{2.5}$ concentration over China from Dec. 2014 to Nov. 2015 for winter (Dec.-Jan.-Feb., or DJF), spring (Mar.-Apr.-May, or MAM), summer (Jun.-Jul.-Aug., or JJA) and autumn (Sep.-Oct.-Nov., or SON) [4]. The tiny figure at the bottom-right corner is the Nine-Dash Line of China.

Results. − We calculate firstly the mean $PM_{2.5}$ concentration $\langle X_i \rangle = \frac{1}{T}\sum_{t=1}^{T} X_i(t)$ of sites $i = 1, 2, \ldots, 163$ and show them in fig. 1 for the four seasons. The overall average

$$\bar{X} = \frac{1}{N}\sum_{i=1}^{N}\langle X_i \rangle \qquad (7)$$

is $75.3\,\mu\mathrm{g/m^3}$ in winter, $48.2\,\mu\mathrm{g/m^3}$ in spring, $36.5\,\mu\mathrm{g/m^3}$ in summer and $46.9\,\mu\mathrm{g/m^3}$ in autumn. In winter, 45 percent of sites has mean $PM_{2.5}$ concentration above $75\,\mu\mathrm{g/m^3}$ and the percentage of the sites above $35\,\mu\mathrm{g/m^3}$ is 95%. The maximum mean $PM_{2.5}$ concentration in winter is related to the enhanced anthropogenic emissions from fossil fuel combustion, biomass burning and unfavorable meteorological conditions for pollution dispersion [4]. In spring, 8 percent of sites have mean concentrations above $75\,\mu\mathrm{g/m^3}$ and 77 percent are above $35\,\mu\mathrm{g/m^3}$. The lowest mean $PM_{2.5}$ concentration is reached in summer. Only 4 percent of sites have mean concentrations above $75\,\mu\mathrm{g/m^3}$ and 47 percent are above $35\,\mu\mathrm{g/m^3}$. In autumn, the percentage of sites above $35\,\mu\mathrm{g/m^3}$ and $75\,\mu\mathrm{g/m^3}$ reaches 78% and 7%, respectively.

The cross-correlation functions $\hat{C}_{ij}(\tau)$ between N sites were calculated according to eq. (1) and with $\tau_{max} = 10$ days. From $\hat{C}_{ij}(\tau)$, we can obtain the correlation C_{ij} between sites i and j. The PDF $\rho(C)$ of correlation is presented in fig. 2 for the four seasons. It can be seen that $\rho(C)$ is separated into positive and negative parts (corresponding to $C > 0$ and $C < 0$, respectively).

The proportions of positive and negative correlations can be calculated by

$$\lambda_p = \int_0^1 \rho(C)\mathrm{d}C, \qquad (8)$$

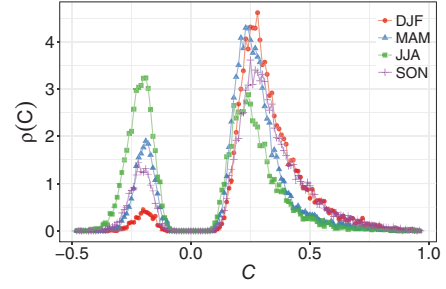$$\lambda_n = \int_{-1}^0 \rho(C)\mathrm{d}C. \qquad (9)$$

Fig. 2: (Color online) Probability distribution function of correlation between sites in the four seasons from Dec. 2014 to Nov. 2015.
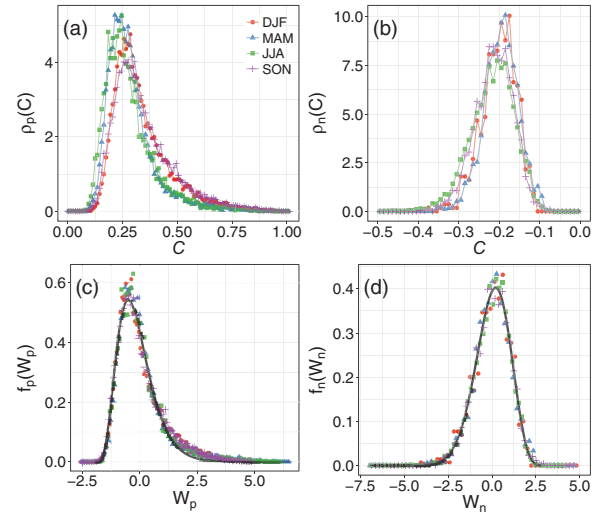

Fig. 3: (Color online) Probability distribution functions $\rho_p(C)$ in (a) and $\rho_n(C)$ in (b). The variation of $f(W)$ as a function of the scaling quantity W for (c) positive and (d) negative correlations.

For positive correlations, we get $\lambda_p = 95\%$ in winter, 78% in spring, 55% in summer and 84% in autumn. Correspondingly, the negative correlations have the proportion $\lambda_n = 1 - \lambda_p = 5\%$, 22%, 45% and 16% in the four seasons.

Further, we introduce the probability distribution functions

$$\rho_p(C) = \frac{1}{\lambda_p}\rho(C) \qquad (10)$$

for $C > 0$ and

$$\rho_n(C) = \frac{1}{\lambda_n}\rho(C) \qquad (11)$$

for $C < 0$. They are presented in fig. 3(a) and (b) and depend on the season. The averages $\langle C_p \rangle$, $\langle C_n \rangle$ and standard deviations σ_p, σ_n of positive and negative correlations can be calculated with $\rho_p(C)$ and $\rho_n(C)$. Their results are summarized in table 1 for different seasons. λ_p and $\langle C_p \rangle$ have their maximum in winter and minimum in summer, which is in accord with the overall average of mean $PM_{2.5}$ concentration.

In a system near its critical point, its physical properties follow a scaling behavior because of long-range correlation [29,30]. The two-variable function of a physical

Table 1: Proportion, average, and standard deviations of positive and negative correlations.

	DJF	MAM	JJA	SON
λ_p	95%	78%	55%	84%
$\langle C_p \rangle$	0.406	0.361	0.356	0.397
σ_p	0.146	0.136	0.145	0.155
λ_n	5%	22%	45%	16%
$\langle C_n \rangle$	−0.249	−0.255	−0.277	−0.254
σ_n	0.058	0.060	0.072	0.064

property can be rewritten as a function of the scaled variable, which is universal. We take account of the long-range correlation of $PM_{2.5}$ concentration and search for the scaling behavior of the probability distribution functions $\rho_p(C)$ and $\rho_n(C)$. Using the scaling variable

$$W_p = [C - \langle C_p \rangle]/\sigma_p, \qquad (12)$$
$$W_n = [C - \langle C_n \rangle]/\sigma_n, \qquad (13)$$

we can introduce two scaling functions

$$f_p(W_p) = \sigma_p \cdot \rho_p(C) \qquad (14)$$

for positive correlations and

$$f_n(W_n) = \sigma_n \cdot \rho_n(C). \qquad (15)$$

for negative correlations. As shown in fig. 3(c) and (d), the scaling distribution functions for positive and negative correlations in the four seasons collapse together. This indicates that there is the same mechanism behind the correlation of $PM_{2.5}$ concentration.

The different characters of positive and negative correlations can be demonstrated further by their PDF of distance r and time lag τ^*, which are shown in fig. 4. $\rho_p(r)$ of positive correlations has its peak at the PDF of r and τ^* which are shown in fig. 4(a) and (c). The PDF of negative correlations are presented in fig. 4(b) for the distance and in fig. 4(d) for the time lag. At the peaks of PDF, the distance of negative correlations is obviously larger than that of positive correlations. The PDF of time lag has a maximum at $\tau^* = 0$ for positive correlations and $\tau^* \neq 0$ for negative correlations. Negative correlations take on the character of larger distance and longer time lag.

The average positive correlation $\bar{C}_p(r)$ at fixed distance r is shown in fig. 4(e). The decay of $\bar{C}_p(r)$ follows a power law in some range of r. A linear fitting process is applied in log-log data. Since the head and tail data should not satisfy the power law, we intercepted the data in the middle to fit. The power-law slopes are -0.48 ± 0.009, -0.52 ± 0.03, -0.59 ± 0.05 and -0.49 ± 0.01 for DJF, MAM, JJA and SON. The power-law slope decays slowest in winter and the fitting error is minimal. This could be related to the transport of $PM_{2.5}$ by atmospheric currents. This trend will be weakened in summer [31]. The average negative correlation $\bar{C}_n(r)$ demonstrates quite different behaviors,
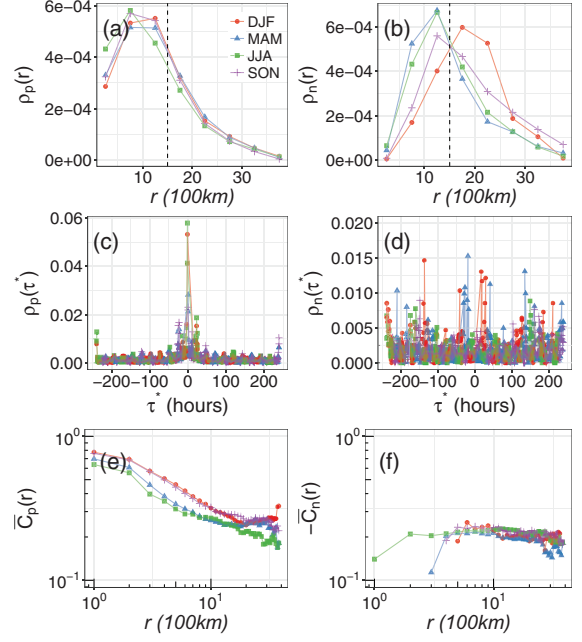

Fig. 4: (Colour online) The PDF of the distance r is shown in (a) for positive and in (b) for negative correlations. The PDF of time lag τ^* is shown in (c) for positive and in (d) for negative correlations. Averages of positive and negative correlations at distance r are plotted in (e) and (f).
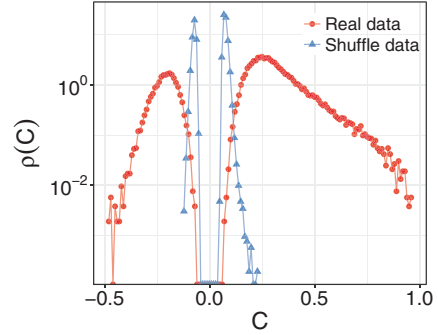

Fig. 5: (Color online) PDF of correlations from real data and shuffle data in all seasons.

which are shown in fig. 4(f). At large distance, $\bar{C}_n(r)$ becomes nearly constant. We suppose that negative correlations are the result of some external factors existing in a large scale of distance, *i.e.*, the large-scale atmospheric waves or oscillations.

To define the correlation network, the threshold Δ of the correlation is determined from the shuffled data obtained by permuting randomly the real data in a season. The PDF of the correlation from shuffle data is compared with that from real data in fig. 5. We define the average of absolute values of correlations from shuffled data as the threshold Δ. We obtain $\Delta = 0.017$ and the adjacency matrix of the network for correlation C according to eq. (2).

The weighted degree of a site, which characterizes its total correlation with surrounds, can be calculated using
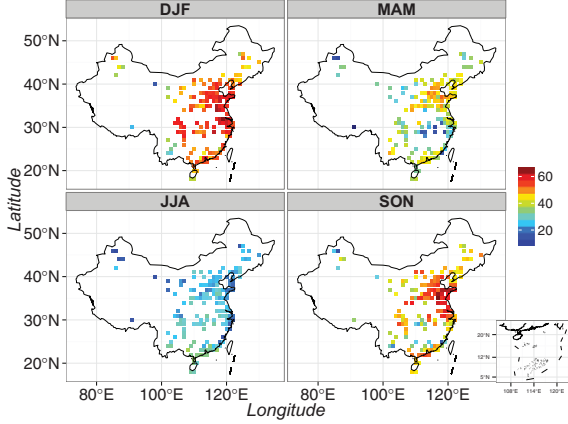
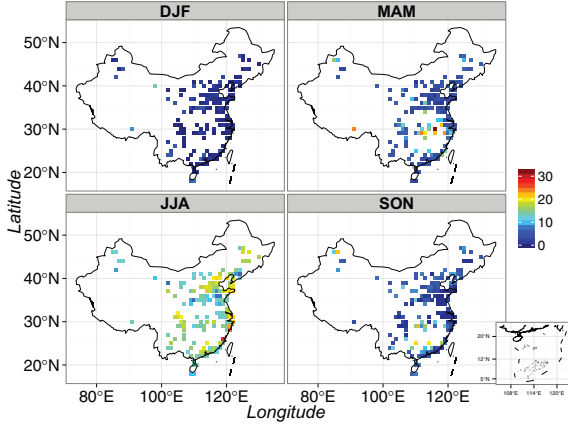Fig. 6: (Color online) Distribution of weighted degree in the network of positive correlations.

Fig. 8: (Color online) Distribution of directional degree in the network of positive correlations.

Fig. 7: (Color online) Distribution of weighted degree in the network of negative correlations.

Fig. 9: (Color online) Distribution of directional degree in the network of negative correlations.

eq. (3). The distribution of the weighted degree for positive correlations is shown in fig. 6. In comparison with fig. 1 of mean $PM_{2.5}$ concentration, the relevance of the weighted degree to mean $PM_{2.5}$ concentration can be found. In the regions with larger mean $PM_{2.5}$ concentration, the sites there have also a larger weighted degree. The weighted degrees are also larger in winter than in other seasons.

For negative correlations, distributions of weighted degree in different seasons are shown in fig. 7. On the contrary, there are the largest weighted degrees in summer and the smallest weighted degrees in winter.

The directional degree of a site, which is calculated according to eq. (4), characterizes its net influence to the surroundings. We present the distribution of the directional degree for positive correlations in fig. 8. In winter, there are the strongest directional degrees in the most sites. The sites of the north-west China, such as Xinjiang, Sichuan and Guizhou, have directional degrees in the direction from west to east. The directional degrees indicate net influences of $PM_{2.5}$ concentration along Gobi and Inner Mongolia plateau, the North China Plain, Central
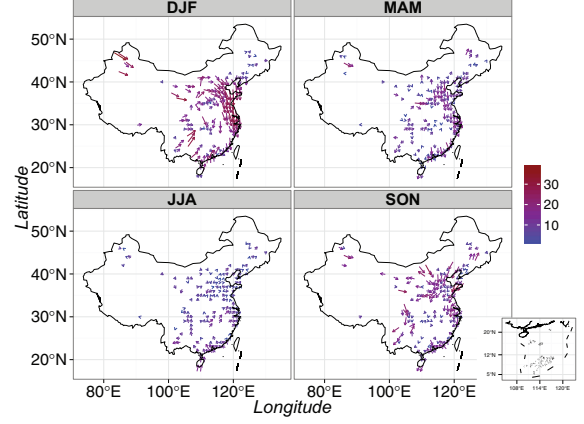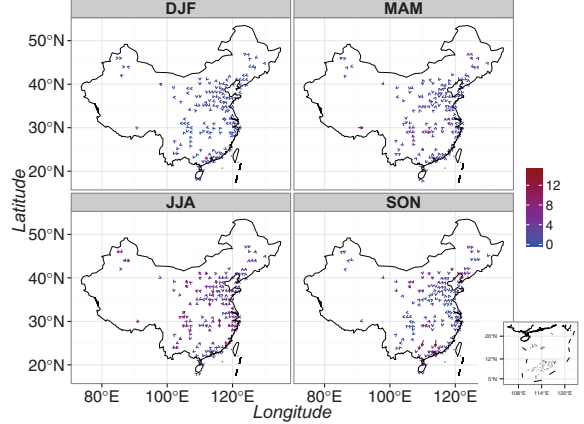
China, and Yangtze River Delta. These phenomena can be related to the east Asia winter monsoon [31,32], which has been shown by numerous studies. In other seasons, the directional degrees are smaller and less directional than in winter. In summer especially, only the sites around Pearl River Delta have visible directional degrees in the direction from south to north. The distribution of the directional degree for negative correlations is shown in fig. 9. No significant directional influence can be found for negative correlations.

According to eq. (5), G_{ij} between sites i and j can be calculated. The threshold $\Theta = 3.25$ of G can be obtained by averaging absolute values of the shuffled data of G. It is found that Θ is larger than all absolute values of negative G_{ij}. Therefore, only a network of positive G_{ij} can be defined by the adjacency matrix B of eq. (6) . The paper [27] has discussed the characteristics of G and C in details by using surface air temperature data. They found that the major differences between the two networks are caused by the autocorrelation in the records. Two correlated high-frequency signals will correspond to a large $|G|$. But for the correlated low-frequency signals could get a large $|C|$
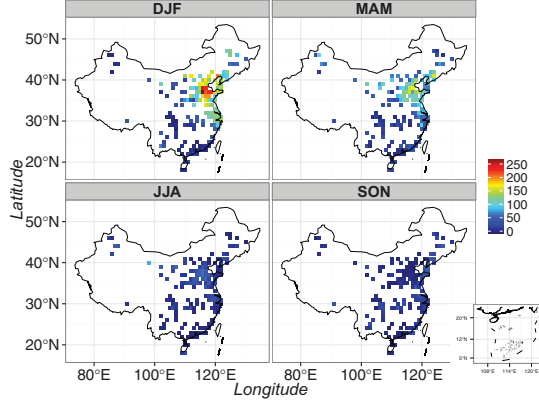
Fig. 10: (Color online) Distribution of positive weighted degree G in the network.
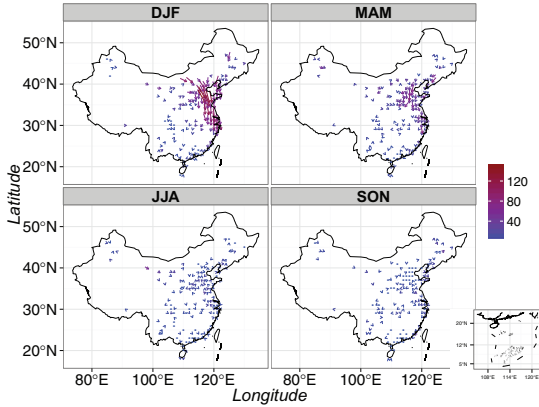

Fig. 11: (Color online) Distribution of positive directional weighted degree G in the network.

with small $|G|$. Thus, the negative part with small $|G|$ is mainly produced by low frequency signals. For the positive part, the distribution of weighted degree in this G network is shown in fig. 10. The weighted degrees in summer and autumn are close to zero. In winter and spring, there are large weighted degrees in the eastern part of China, especially around Beijing. The distribution of directional degrees of the G network is shown in fig. 11. We can also see that there are large directional degrees only in winter and spring and in the eastern part of China, as well as the weighted degrees. The direction of directional degrees is from north to south. We think that the large weighted and directional degrees of the G network are the result of the high-frequency process of cold fronts with strong winds which help to ventilate $PM_{2.5}$ in heavily polluted regions. Comparing with fig. 6 and fig. 8, some weighted and directional degrees become small in the western part of China. This implies that their degrees are not due to strong winds, but are caused by some low-frequency factors such as transport by the difference in terrain height. With the C and G networks, different properties of $PM_{2.5}$ concentration in China have been found.

Summary. – We have studied the correlations of $PM_{2.5}$ concentrations in different sites of China. Using the hourly $PM_{2.5}$ concentration data in 754 monitoring sites over China from Dec. 2014 to Nov. 2015, we can calculate correlations between different sites in the four seasons. The probability distribution functions of positive and negative correlations depend on season. With averages and standard deviations of correlation, the different probability distribution functions of the different seasons can be scaled into one scaling function. This indicates that there is maybe the same mechanism related to the correlation of $PM_{2.5}$ concentration in different seasons. But positive and negative correlations are quite different corresponding to different atmospheric processes.

Further, $PM_{2.5}$ concentrations in different sites of China are studied from the aspect of complex networks. Networks of $PM_{2.5}$ concentration can be defined either by correlations or by their significances. By using weighted and directional degrees of network, different properties of $PM_{2.5}$ concentration can be studied. In the networks of positive correlations, the largest weighted degrees appear in winter and in the North China Plain as far as location is concerned. The location distribution of the weighted degree and its seasonal dependence are in accord with that of the mean $PM_{2.5}$ concentration. In the networks of negative correlations, the largest weighted degrees appear in summer. This indicates further that the origins of positive and negative correlations are different. Positive correlations are mainly caused by transmission of $PM_{2.5}$. In winter, this effect is most remarkably related to the global serious air pollution and the direction of transmission is affected by wind in eastern China. In summer this effect is very weak. Instead, negative correlations dominate. Negative correlations are caused probably by large-scale oscillating climate conditions, *i.e.*, the large-scale atmospheric waves. Based on significances of positive correlation G, we can find the correlated high-frequency signals only in winter and spring and in the eastern part of China. The directional degrees are in the direction from north to south. These properties of $PM_{2.5}$ concentrations could be related to cold fronts with strong winds which help to ventilate $PM_{2.5}$ in heavily polluted regions.

* * *

council. We also acknowledge the data resources provided by the ministry of environmental protection of China (`http://113.108.142.147:20035/emcpublish/`).

REFERENCES

[1] Chen Y., Ebenstein A., Greenstone M. and Li H., *Proc. Natl. Acad. Sci. U.S.A.*, **110** (2013) 12936.
[2] Cao J. J., Lee S. C., Ho. K. F., Zhang X. Y., Zou S. C., Fung K., Chow J. C. and Watson J. G., *Atmos. Environ.*, **37** (2003) 1451.
[3] Cao J. J., Shen Z. X., Chow J. C., Watson J. G., Lee S. C., Tie X. X., Ho K. F., Wang G. H. and Han Y. M., *J. Air Waste Manag. Assoc.*, **62** (2012) 1214.
[4] Zhang Y. L. and Cao F., *Sci. Rep.*, **5** (2015) 14884.
[5] Hu J. L., Wang Y., Ying Q. and Zhang H., *Atmos. Environ.*, **95** (2014) 598.
[6] Gao H., Chen J., Wang B., Tan S., Lee C., Yao X. and Yan H., *Atmos. Environ.*, **45** (2011) 3069.
[7] Zhang J. P., Zhu T., Zhang Q. H., Li C. C., Shu H. L., Ying Y., Dai Z. P., Wang X., Liu X. Y., Liang A. M., Shen H. X. and Yi B. Q., *Atmos. Chem. Phys.*, **12** (2012) 5031.
[8] Xie Y., Zhao B., Zhang L. and Luo R., *Particuology*, **20** (2015) 141.
[9] Xu W. Y., Zhao C. S., Ran L., Deng Z. Z., Liu P. F., Ma N., Lin W. L., Xu X. B., Yan P., He X., Yu J., Liang W. D. and Chen L. L., *Atmos. Chem. Phys.*, **11** (2011) 4353.
[10] Chen D., Zhang Y. W. and Tie X., *Sci. Sin. Phys. Mech. Astron.*, **47** (2017) 020501.
[11] Boccaletti S., Latora V., Moreno Y., Chavez M. and Hwang D., *Phys. Rep.*, **424** (2006) 175.
[12] Girvan M. and Newman M. E. J., *Proc. Natl. Acad. Sci. U.S.A.*, **99** (2002) 7821.
[13] Cohen R. and Havlin S., *Complex Networks: Structure, Robustness and Function* (Cambridge University Press, Cambridge, England) 2010.
[14] Wiedermann M., Radebach A., Donges J. F., Kurths J. and Donner R. V., *Geophys. Res. Lett.*, **43** (2016) 7176.
[15] Boers N., Bookhagen B., Marwan N., Kurths J. and Marengo J., *Geophys. Res. Lett.*, **40** (2010) 4386.
[16] Ludescher J., Gozolchiani A., Bogachev M. I., Bunde A., Havlin S. and Schellnhuber H. J., *Proc. Natl. Acad. Sci. U.S.A.*, **111** (2014) 2064.
[17] Tsonis A. A. and Swanson K. L., *Phys. Rev. Lett.*, **100** (2008) 228502.
[18] Yamasaki K., Gozolchiani A. and Havlin S., *Phys. Rev. Lett.*, **100** (2008) 228501.
[19] Wang Y., Gozolchiani A., Ashkenazy Y., Berezin Y., Guez O. and Havlin S., *Phys. Rev. Lett.*, **111** (2013) 138501.
[20] Wang Y., Gozolchiani A., Ashkenazy Y. and Havlin S., *New J. Phys.*, **18** (2016) 033021.
[21] Berezin Y., Gozolchiani A., Guez O. and Havlin S., *Sci. Rep.*, **2** (2012) 666.
[22] Boers N., Bookhagen B., Marwan N., Kurths J. and Marengo J., *Geophys. Res. Lett.*, **40** (2013) 4386.
[23] Boers N., Bookhagen B., Barbosa H. M., Marwan N., Kurths J. and Marengo J., *Nat. Commun.*, **5** (2014) 5199.
[24] Donges J. F., Zou Y., Marwan N. and Kurths J., *Eur. Phys. J. ST*, **174** (2009) 157.
[25] Donges J. F., Zou Y., Marwan N. and Kurths J., *EPL*, **87** (2009) 48007.
[26] Runge J., Petoukhov V., Donges J. F., Hlinka J., Jajcay N., Vejmelka M., Hartman D., Marwan N., Palus M. and Kurths J., *Nat. Commun.*, **6** (2015) 8502.
[27] Guez O. C., Gozolchiani A. and Havlin S., *Phys. Rev. E*, **90** (2014) 062814.
[28] Fan J. F., Meng J., Ashkenazy Y., Havlin S. and Schellnhuber H. J., *Proc. Natl. Acad. Sci. U.S.A.*, **114** (2017) 201701214.
[29] Li X. T. and Chen X. S., *Commun. Theor. Phys.*, **66** (2016) 355.
[30] Fan J. F., Liu M. X., Li L. S. and Chen X. S., *Phys. Rev. E*, **85** (2012) 61110.
[31] Lau W. K. M., *J. Meteorol. Res.*, **30** (2016) 1.
[32] Li Q., Zhang R. and Wang Y., *Int. J. Climatol.*, **36** (2015) 346.